Polymer Chemistry

PAPER

Check for updates

Synthesis of megadalton stereoregular ring-substituted poly(phenylacetylene)s by a rhodium(I) catalyst with a N-functionalized hemilabile phosphine ligand†

Marta Angoy, M. Victoria Jiménez, [ID] * Eugenio Vispe [ID] and Jesús J. Pérez-Torrente [ID] *

The cationic compound [Rh(nbd){$\kappa^2 P,N$-Ph$_2$P(CH$_2$)$_3$NMe$_2$}][BF$_4$] efficiently catalyzes the polymerization of a series of ring-substituted phenylacetylene derivatives, R-C$_6$H$_4$–C≡CH with groups of different electronic and steric properties at the *para* (R = F, CF$_3$, Me, Bu, ^{t}Bu, OMe, OBu) and *meta* (R = OMe) positions to give highly stereoregular ring-substituted poly(phenylacetylene)s with a *cis*-transoidal configuration of very high molar mass and moderate dispersities. The polymers have been characterized by size exclusion chromatography (SEC-MALS), NMR, DSC and TGA. The polymerization of phenylacetylene and 1-ethynyl-3-methoxybenzene gives megadalton poly(phenylacetylene)s, while the polymerization of 1-ethynyl-4-methoxybenzene and 1-(*tert*-butyl)-4-ethynylbenzene gives ultra-high molecular weight poly(phenylacetylene)s with M_n of 1.70×10^6 and 2.72×10^6, respectively. The electronic effect of the substituent strongly influences the catalytic activity. Phenylacetylene derivatives with an electron-withdrawing substituent in *para* position polymerize faster than those with an electron-donating substituent.

Introduction

Conjugated polymers have attracted significant attention due to their use as conductive polymers for optoelectronics and energy applications.[1–3] In particular, poly(phenylacetylene) (PPA) has been intensively studied due to its stability in air, high solubility in common organic solvents, excellent processability and semiconducting properties.[4,5] The wide choice of substituted phenylacetylene (PA) derivatives has provided access to functional polymers with applications in electronics, photoelectronics, optics, and membrane separation.[6–8] Furthermore, a range of supramolecular assemblies derived from PPAs have been prepared, including nanoparticles, nanotubes, gels, liquid crystals, fibers, and composites.[9]

The processing behavior and many of the end-use properties of polymers are influenced by the molecular weight and molecular weight distribution (MWD). Therefore, control of both parameters is essential to tailor polymers to meet specific application requirements.[10] Ultrahigh-molecular

weight (UHMW) polymer materials offer improved physical and mechanical properties. Consequently, the development of synthetic methods for UHMW polymers, *i.e.* polymers with a number-average molecular weight (M_n) greater than 10^6 g mol^{-1}, is an interesting research topic in polymer chemistry.[11–14] In addition to molecular weight, the stereochemistry and conformation of PPAs also influence their chemical and physical properties.[15]

Although a number of transition metal catalysts are available for the polymerization of phenylacetylene derivatives, those based on late transition metals such as ruthenium, rhodium, iridium and palladium have attracted considerable attention due to their high activity, stability to air and moisture, and high tolerance to many of the heteroatoms in alkyne-functionalized monomers.[16] In particular, rhodium catalysts efficiently catalyze the polymerization of phenylacetylene derivatives to give highly stereoregular polymers with *cis*-transoidal conformation.[17,18] Recently, significant progress has been made in the design of rhodium(I) catalysts for the living polymerization of alkyne-based monomers.[19–21] Well-defined Rh-alkynyl,[22,23] Rh–vinyl,[24–26] and Rh–aryl,[27–29] complexes allow the controlled (co)polymerization of PA derivatives to give highly stereoregular (co)polymers with narrow MWD and very high initiation efficiencies. However, moderate to high molecular weight PPAs have typically been obtained.

Departamento de Química Inorgánica, Instituto de Síntesis Química y Catálisis Homogénea–ISQCH, Universidad de Zaragoza–CSIC, Facultad de Ciencias, C/Pedro Cerbuna, 12, 50009 Zaragoza, Spain. E-mail: perez@unizar.es, vjimenez@unizar.es
†Electronic supplementary information (ESI) available: NMR spectra, SEC-MALS chromatograms and DSC thermograms of PPAs. Kinetic data for the PA polymerization reactions. See DOI: https://doi.org/10.1039/d4py00259h

The number of rhodium-based catalytic systems leading to ultrahigh-molecular weight PPAs is rather limited (Chart 1). Some time ago, Tabata *et al.* reported that the PA polymerization activity of the rhodium dimer $[Rh(\mu\text{-}Cl)(nbd)]_2$ (nbd = 2,5-norbornadiene) could be significantly enhanced in polar solvents such as triethylamine, alcohol, water, and THF.[30] Indeed, PA polymerization in triethylamine afforded stereoregular ultrahigh-molecular weight PPA, M_w up to 4.43×10^6, albeit in low yield. More recently, Bielawski *et al.* reported a heterogeneous catalyst based on a rhodium(I) polymer, $[Rh_2(\mu\text{-}Cl)_2(\text{cyclooctatetraene})]_n$, supported on silica. In the presence of an external base, triethylamine, ultrahigh-molecular weight PPA, M_n up to 1.29×10^6, was produced in a stereoselective manner.[31] Our research group has developed a complementary strategy for the design of efficient rhodium(I) PA polymerization catalysts based on the utilization of functionalized ligands with the ability to act as an internal base. In particular, the mononuclear phosphino-anilido $[Rh(nbd)\{\kappa^2 P,N\text{-}Ph_2P(C_6H_4)NMe\}]$ complex efficiently catalyzed the polymerization of PA to yield ultrahigh-molecular weight PPA with M_n up to 1.94×10^6.[32]

Following this strategy, we have prepared a series of rhodium(I) catalysts based on N-functionalized phosphine ligands of hemilabile character (Chart 2). Cationic rhodium(I) complexes containing amino-functionalized phosphine ligands, such as $[Rh(nbd)\{\kappa^2 P,N\text{-}Ph_2P(CH_2)_3NR_2\}]^+$ (R = H, Me) and $[Rh(nbd)\{\kappa^2 P,N\text{-}Ph_2P(C_6H_4)NHMe\}]^+$, efficiently catalyzed PA polymerization leading to stereoregular megadalton PPAs (M_n in the range $1.1\text{–}1.5 \times 10^6$) with moderate dispersity.[32,33] Similarly, neutral complexes with amino-functionalized N-heterocyclic carbene ligands, $[RhCl(nbd)\{\kappa C\text{-}MeIm(CH_2)_3NMe_2\}]$ and $[RhBr(nbd)\{\kappa C\text{-}MeIm(CH_2)_3NH_2\}]$, or pyridine-functionalized phosphino ligands, such as $[RhCl(nbd)\{\kappa P\text{-}Ph_2P(CH_2)_2Py\}]$, also yielded megadalton PPAs with M_n of about 1.3×10^6.[34]

The aim of this work is to evaluate the potential of the catalyst $[Rh(nbd)\{\kappa^2 P,N\text{-}Ph_2P(CH_2)_3NMe_2\}][BF_4]$.[35] in the polymerization of a series of ring-substituted phenylacetylene derivatives with different electronic and steric properties for the preparation of very high molecular weight PPAs. The choice of the 3-(dimethylamino-propyl)diphenylphosphine ligand is based on both the ease of its preparation[36] and the catalytic performance of cationic rhodium-diene catalysts with this hemilabile ligand, which exhibit excellent PA conversions in short reaction times, resulting in the formation of megadalton PPA polymers.

Chart 2 Molecular catalysts for phenylacetylene polymerization leading to megadalton PPAs ($M_n = 1.1\text{–}1.5 \times 10^6$).

Experimental section

Materials

All experiments were carried out under an atmosphere of argon using Schlenk techniques or glovebox. Solvents were distilled immediately prior to use from the appropriate drying agents or obtained from a Solvent Purification System (Innovative Technologies). The terminal arylacetylenes: phenylacetylene (**PAa**), 1-ethynyl-3-methoxybenzene (**PAf**), 1-butoxy-4-ethynylbenzene (**PAh**) (Merck), and 1-ethynyl-4-fluorobenzene (**PAb**), 1-ethynyl-4-methylbenzene (**PAc**), 1-ethynyl-4-(trifluoromethyl)benzene (**PAd**), 1-ethynyl-4-methoxybenzene (**PAe**), 1-butyl-4-ethynylbenzene (**PAg**), 1-(*tert*-butyl)-4-ethynylbenzene (**PAi**) (Acros Organics), were distilled over CaH_2 under reduced pressure and stored over molecular sieves.

Methods

The absolute molecular weight averages (M_n and M_w), dispersity ($Đ$, M_w/M_n) and molecular weight distribution were determined by SEC-MALS at the Chromatography and Spectroscopy Service of the ISQCH. SEC-MALS analyses were carried out using a Waters 2695 instrument, equipped with three PL-Gel Mixed B LS columns fitted to a MALS detector (MiniDawn Treos, Wyatt) and a differential refractive index detector (Optilab Rex, Wyatt). The polymer solutions in THF (≈ 2.0 mg mL^{-1}) were filtered through a 0.45 μm PTFE membrane filter before being injected in the GPC systems. The analyses were carried out immediately after the dissolution

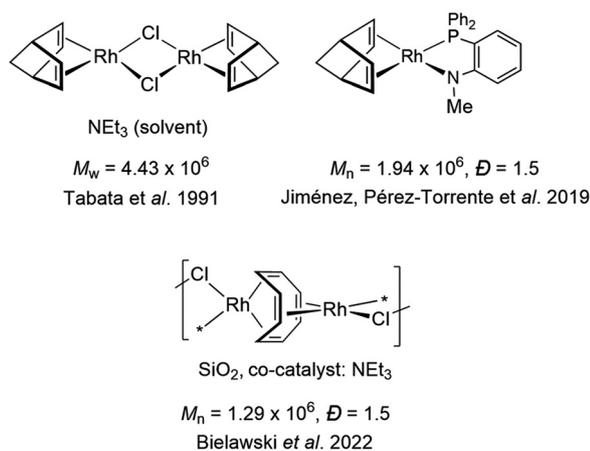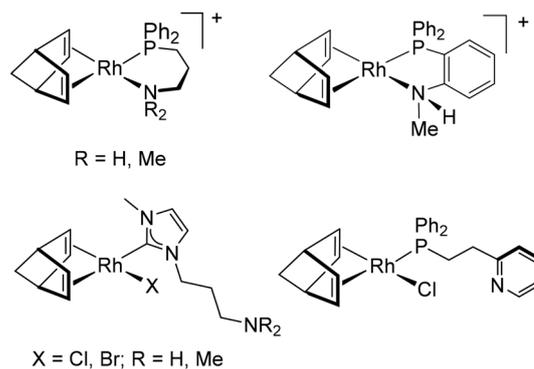**Chart 1** Catalytic systems for phenylacetylene polymerization leading to ultrahigh-molecular weight (UHMW) PPA.

of the polymer sample in THF to minimize sample degradation.[37,38] Data analysis was performed with ASTRA Software from Wyatt. Polymer samples were eluted at 25 °C with THF at a flow rate of 1.0 mL min^{-1}. The dn/dc parameter in THF at 658 nm was determined for each polymer using the full mass recovery method, which assumes 100% recovery of the injected mass of a polymer sample of known concentration,[39] except for **PPAe** and **PPAh** which exhibited poor mass recovery due to insoluble species and therefore the dilution method was used (five samples from 0.1 mg mL^{-1} to 10 mg mL^{-1} were analyzed). The polymers **PPAa**, **PPAb** and **PPAi** were completely soluble. Other polymers were difficult to dissolve, resulting in mass recoveries of 90% for **PPAg** and **PPAf**, 65% for **PPAe** and 75% for **PPAh**. The dn/dc values of **PAa**, **PAb**, **PAe**, **PAf**, **PAg**, **PAh**, and **PAi**, were determined to be 0.286, 0.210, 0.258, 0.265, 0.231, 0.261, and 0.224 mL g^{-1}, respectively. The poor solubility of **PAc** and **PAd** precluded dn/dc determination and molar mass measurement.

^{1}H NMR spectra were recorded on a Bruker Avance 300 or 400 spectrometers. NMR chemical shifts are reported in ppm relative to tetramethylsilane and referenced to partially deuterated solvent resonances. Coupling constants (J) are given in Hertz. Thermal gravimetric analyses were carried out on a TA Q-5000 TGA apparatus (TA Instruments). Samples were heated under nitrogen from room temperature to 600 °C at a rate of 10 °C min^{-1}, and then up to 750 °C on air at the same rate. Differential scanning calorimetry experiments were carried out on a DSC Q-20 apparatus (TA Instruments). Samples were heated under nitrogen from 20 °C to 200 °C at a rate of 10 °C min^{-1} and cooled to the initial temperature at the same rate. In some experiments this cycle was repeated several times. DSC plots are shown in exo-down mode. Chromatographic analysis was performed on an HP 5890 Series II gas chromatograph with ionization detector and an HP-5 column (25 m × 0.32 mm i.d. × 0.17 μm). Calibration of the detector response to the different alkynes was carried out using n-octane as internal standard.

Synthesis of catalyst [Rh(nbd){κ^2P,N-Ph$_2$P(CH$_2$)$_3$NMe$_2$}][BF$_4$][35]

AgBF$_4$ (169 mg, 0.868 mmol) was added to a suspension of [Rh(μ-Cl)(nbd)]$_2$ (200 mg, 0.434 mmol) in tetrahydrofuran (10 mL). The resulting suspension was stirred for 30 min and the formed AgCl filtered off and washed with 3 tetrahydrofuran (3 × 1 mL). The volume of the resulting yellow solution, containing the solvated species [Rh(nbd)(THF)$_n$]$^+$, was reduced to about 5 mL and then a solution of the phosphine Ph$_2$P(CH$_2$)$_3$NMe$_2$ (235 mg, 0.868 mmol) in tetrahydrofuran (2 mL) was slowly added at 0 °C to give an orange solution. Concentration of the solution to about 0.2 mL and slow addition of diethyl ether (5 mL) afforded the compound as an orange solid which was washed with diethyl ether (3 × 2 mL) and dried under vacuum. Yield: 61%. ^{1}H NMR (298 K, CDCl$_3$): δ 7.58–7.42 (m, 10H, Ph), 5.31 (br, 2H, =CH cod), 3.14 (br, 2H, =CH cod), 2.86 (br, 2H, CH$_2$N), 2.40 (m, 6H; 4H CH$_2$ cod, 2H CH$_2$), 2.34 (s, 6H,

NMe$_2$), 1.94 (m, 6H; 4H CH$_2$ cod, 2H CH$_2$). ^{31}P{^{1}H} NMR (298 K, CDCl$_3$): δ 17.92 (d, $J_{P–Rh}$ = 155.7).
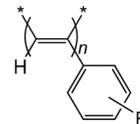
Polymer synthesis and characterization

The polymerization reactions were carried out in round bottom flasks with efficient stirring. A typical polymerization procedure is as follows: terminal aryl alkyne (0.64 mmol) was added to a THF solution (2.5 mL) of the catalysts (6.4 μmol) and the mixture stirred at 293 K in the absence of light. The consumption of monomer was monitored by GC using octane as internal standard. The polymer solutions were transferred into vigorously stirred cold methanol (25 mL, 273 K) using a cannula under argon. The polymers were filtered, washed with methanol (3 × 5 mL) and dried under vacuum to constant weight. The polymers were obtained as yellow-orange solids in good yields according to the attained conversion values.

NMR data

PPAa (R = H). ^{1}H NMR (298 K, 300 MHz, CD$_2$Cl$_2$): δ 6.98 (d, 3H), 6.67 (t, 2H), 5.85 (s, 1H, =CH). ^{13}C{^{1}H} NMR (298 K, 300 MHz, CD$_2$Cl$_2$): δ 142.9, 139.4 (C$_q$), 131.8 (=CH), 127.8, 127.6, 126.7 (CH). **PPAb** (R = p-F). ^{1}H NMR (298 K, 300 MHz, CDCl$_3$): δ 6.67 (m, 4H), 5.72 (s, 1H, =CH). ^{13}C{^{1}H} NMR (298 K, 400 MHz, CDCl$_3$): δ 163.9, 161.5, 139.3 (C$_q$), 131.5 (=CH), 129.3 (CH, $J_{C–F}$ = 8 Hz), 113.3 (CH, $J_{C–F}$ = 48 Hz). **PPAe** (R = p-OMe). ^{1}H NMR (298 K, 300 MHz, CDCl$_3$): δ 6.96 (m, 2H), 6.70 (d, 2H), 5.91 (s, 1H, =CH), 3.59 (s, 3H, OMe). ^{1}H NMR (298 K, 400 MHz, CD$_2$Cl$_2$): δ 6.65 (d, 2H), 6.48 (d, 2H), 5.76 (s, 1H, =CH), 3.58 (s, 3H, OMe). ^{13}C{^{1}H} NMR (298 K, 400 MHz, CD$_2$Cl$_2$): δ 158.9, 139.1, 136.0 (C$_q$), 128.9 (=CH), 127.8, 113.3 (CH), 55.32 (OMe). **PPAf** (R = m-OMe). ^{1}H NMR (298 K, 300 MHz, CDCl$_3$): δ 6.83 (t, 1H), 6.52 (d, 1H), 6.29 (d, 2H), 6.26 (s, 1H), 5.85 (s, 1H, =CH), 3.56 (s, 3H, OMe). ^{1}H NMR (298 K, 300 MHz, CD$_2$Cl$_2$): δ 6.85 (t, 1H), 6.55 (d, 1H), 6.30 (d, 1H), 6.28 (s, 1H), 5.85 (s, 1H, =CH), 3.56 (s, 3H, OMe). ^{13}C{^{1}H} NMR (298 K, 300 MHz, CD$_2$Cl$_2$): δ 159.1, 144.2, 139.3 (C$_q$), 131.6 (=CH), 128.6, 120.4, 112.7, 112.3 (CH), 55.0 (OMe). **PPAg** (R = p-Bu). ^{1}H NMR (298 K, 300 MHz, CDCl$_3$): δ 6.70 (d, 2H), 6.54 (d, 2H), 5.73 (s, 1H, =CH), 3.69 (m, 2H, –OCH$_2$), 1.63 (m, 2H, >CH$_2$), 1.39 (m, 2H, >CH$_2$), 0.91 (t, 3H, –CH$_3$). ^{13}C{^{1}H} NMR (298 K, 400 MHz, CDCl$_3$): δ 142.0, 138.5 (C$_q$), 130.1 (=CH), 128.7, 127.0 (CH), 35.2, 33.5, 22.1 (>CH$_2$), 13.7 (–CH$_3$). **PPAh** (R = p-OBu). ^{1}H NMR (298 K, 300 MHz, CD$_2$Cl$_2$): δ 6.60 (d, 2H), 6.43 (d, 2H), 5.73 (s, 1H, =CH), 2.39 (m, 2H, >CH$_2$), 1.44 (m, 2H, >CH$_2$), 1.27 (m, 2H, >CH$_2$), 0.89 (t, 3H, –CH$_3$). ^{13}C{^{1}H} NMR (298 K, 300 MHz, CD$_2$Cl$_2$): δ 158.2, 138.8, 135.7 (C$_q$), 130.1 (=CH), 128.7, 113.5 (CH), 67.7, 31.4, 19.3 (>CH$_2$), 13.7 (–CH$_3$). **PPAi** (R = p-^{t}Bu). ^{1}H NMR (298 K, 300 MHz, CDCl$_3$): δ 6.97 (d, 2H), 6.54 (d, 2H), 5.81 (s, 1H, =CH), 1.14 (s, 9H, ^{t}Bu).

^{13}C{^{1}H} NMR (298 K, 400 MHz, CDCl$_3$): δ 148.8, 140.4, 138.8 (C$_q$), 127.1 (=CH), 126.8, 124.3 (CH), 40.6 (C$_q$ ^{t}Bu) 31.2 (^{t}Bu).

Results and discussion

Polymerization of ring-substituted phenylacetylene derivatives catalyzed [Rh(nbd){κ^2P,N-Ph$_2$P(CH$_2$)$_3$NMe$_2$}][BF$_4$]

The cationic compound [Rh(nbd){κ^2P,N-Ph$_2$P(CH$_2$)$_3$NMe$_2$}][BF$_4$][35] efficiently catalyzed the polymerization of a series of *para*- and *meta*-substituted phenylacetylene derivatives with groups of different electronic and steric properties to afford megadalton PPAs (Fig. 1).

The polymerization reactions were carried out in THF at 20 °C in the absence of light with a monomer to rhodium, [PA]$_o$/[Rh], ratio of 100. The ring-substituted PPAs were isolated as yellow solids in practically quantitative yields according to the conversion values. The ^{1}H NMR spectra of the polymers in CDCl$_3$ or CD$_2$Cl$_2$ showed a sharp singlet corresponding to the vinylic protons of the chain in the range δ 5.85–5.72 ppm, indicating a highly stereoregular structure with a *cis*-transoidal configuration.[40,41] The PPAs were characterized by size exclusion chromatography (SEC) using light-scattering (MALS) and refractive index (DRI) detectors. In general, full PA conversion was achieved in 5–90 min, except in the case of **PAh**

(R = *p*-OBu), to give ring-substituted poly(phenylacetylene)s with very high molar mass (MM) (Table 1).

The obtained ring-substituted PPAs exhibit very high weight-average molar masses, M_w in the range 3.1×10^5–4.8×10^6, and moderate dispersities, $Đ$ in the range 1.4–2.4 (Table 1). A graphical representation of the MMs of the PPA polymers is shown in Fig. 2. Polymerization of the **PAi** (R = *p*-^{t}Bu) monomer was completed in 30 min yielding a fully soluble polymer with a surprisingly high molar mass, M_w of 4.84×10^6, and an initiation efficiency as low as 0.4%. Polymerization of the methoxy-substituted monomers **PAe** (R = *p*-OMe) and **PAf** (R = *m*-OMe) also gave soluble polymers of very high MMs ($M_w \approx 2.0 \times 10^6$). The polymers derived from **PAb** (R = *p*-F) and **PAg** (R = *p*-Bu) showed MMs of around 1.0×10^6. Polymerization of the monomer **PAh** (R = *p*-OBu) was much slower, with only 40% conversion in one hour, yielding the polymer with the lowest molar mass, M_w of 3.12×10^5. The narrowest dispersities were obtained for the polymers **PPAe** (R = *p*-OMe), **PPAg** (R = *p*-Bu) and **PPAh** (R = *p*-OBu) with $Đ$ values of 1.39 and 1.53, respectively. The number-average molecular weight of the polymers (M_n), calculated from the weight-average molecular weight (M_w) and $Đ$, showed the formation of
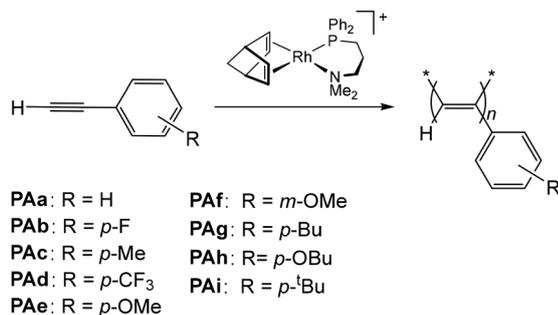

Fig. 1 Polymerization of ring-substituted phenylacetylene derivatives (PAa–PAi) catalyzed by [Rh(nbd){κ^2P,N-Ph$_2$P(CH$_2$)$_3$NMe$_2$}][BF$_4$].
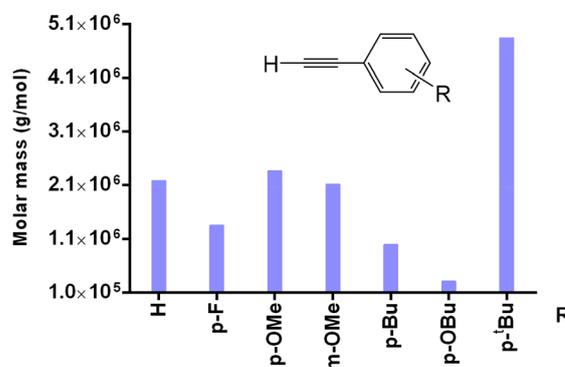

Fig. 2 Molar mass (M_w) of the polymer samples obtained by polymerization of ring-substituted phenylacetylene derivatives catalyzed by [Rh(nbd){κ^2P,N-Ph$_2$P(CH$_2$)$_3$NMe$_2$}][BF$_4$].

Table 1 Polymerization of ring-substituted phenylacetylene derivatives catalyzed by [Rh(nbd){κ^2P,N-Ph$_2$P(CH$_2$)$_3$NMe$_2$}][BF$_4$][a]

				Polymer			
Entry	Mon.	t (min)	Conv.[b] (%)	M_w[c]	$Đ$[c]	M_n[d]	IE[e] (%)
1	**PAa**[f]	60	100	2.18×10^6	2.00	1.09×10^6	0.9
2	**PAb**	30	100	1.35×10^6	2.39	5.65×10^5	1.8
3	**PAc**	60	100	Insoluble			
4	**PAd**	5	100	Insoluble			
5	**PAe**	45	100	2.36×10^6	1.39	1.70×10^6	0.6
6	**PAf**	90	100	2.11×10^6	1.77	1.19×10^6	0.9
7	**PAg**	75	100	9.94×10^5	1.53	6.50×10^5	1.4
8	**PAh**	60	40	3.12×10^5	1.53	2.04×10^5	2.0
9	**PAi**	30	100	4.84×10^6	1.78	2.72×10^6	0.4

[a] Reaction conditions: [PA]$_o$ = 0.25 M, [PA]$_o$/[Rh] = 100, in THF at 293 K. [b] Determined by GC (octane as internal standard). [c] Estimated by SEC-MALS in THF, M_w = weight-average molecular weight (g mol^{-1}), $Đ$ = dispersity (M_w/M_n, M_n = number-average molecular weight). [d] Calculated from M_w and $Đ$, in g mol^{-1}. [e] Initiation efficiency, IE = $M_{theor}/M_n \times 100$; where M_{theor} = [PA]$_o$/[Rh]$_n$MW$_{PA}$ × polymer yield. [f] Ref. 33.

megadalton **PPAa** (R = H) and **PPAf** (R = *m*-OMe) ($M_n \approx 1.1 \times 10^6$), and UHMW **PPAe** (R = *p*-OMe) and **PPAi** (R = *p*-^{t}Bu) polymers, with M_n of 1.70×10^6 and 2.72×10^6, respectively (Table 1).

The polymerization of 1-ethynyl-4-methylbenzene (**PAc**) and 1-ethynyl-4-trifluoromethylbenzene (**PAd**) gave polymers that were insoluble in common solvents such as THF, CHCl$_3$ or toluene, so that their M_w could not be determined. In this context, it has been reported that the polymerization of *ortho*-substituted phenylacetylenes is slower than that of *meta*- and *para*-substituted derivatives and usually leads to insoluble polymers. Analysis of some of these materials by high-angle X-ray scattering (WAXS) revealed highly crystalline materials with a pseudohexagonal network consisting of macromolecules arranged as rods.[42] However, some insoluble polymers derived from *para*-substituted monomers, such as 1-ethynyl-4-chlorobenzene and 1-ethynyl-4-iodobenzene, were found to be almost amorphous materials due to the strong aggregation between the polymer chains.[43] On the other hand, it has already been described that the polymerization of 1-ethynyl-4-methylbenzene leads to the formation of insoluble materials.[44]

The polymers prepared from the ring-substituted phenylacetylene monomers showed a unimodal molecular weight distribution as determined by SEC-MALS analysis (see the ESI†). The ring-substituted PPAs were found to be linear regardless of their molar mass or the characteristics of the substituent. As an example, Fig. 3 shows the MM *vs.* elution volume plot and the log–log plot of the radius of gyration (r_g) *vs.* MM for a **PPAe** sample prepared from **PAe** (R = *p*-OMe). The linearity of the MM plot over the elution volume ranges where both MALS and DRI detectors have detectable intensities, and the linear

relationship of the radius of gyration (r_g) *vs.* the molar mass (MM) in the high molar mass region, is typical of a linear polymer. The slopes of the linear part of the conformation plots, in the range of 0.51–0.63, deviate from the expected value of about 0.58 for a linear polymer reflecting the complex behavior of PPA in dilute solutions due to changes in solvent–polymer and polymer–polymer interactions, as well as the process of σ-*trans* to σ-*cis* isomerization.[45] In sharp contrast, the analysis of the **PPAa** samples obtained by polymerization of phenylacetylene showed the presence of branched polymer with high-MM.[33] In this case, both the deviation from linear behavior in the high-MM region of the log–log plot of r_g *vs.* MM and the detectable increase in the MM in the high-MM region of the MM *vs.* elution volume plot are consistent with branching (see the ESI†).

Light scattering chromatograms and cumulative weight fraction *vs.* molar mass plots for representative polymers are shown in Fig. 4 showing the increase in M_w along the series **PPAh** (R = *p*-OBu, $M_w = 3.12 \times 10^5$), **PPAe** (R = *p*-OMe, $M_w = 2.36 \times 10^6$) and **PPAi** (R = *p*-^{t}Bu, $M_w = 4.84 \times 10^6$).

Time-conversion profiles of PAa–PAi polymerization reactions catalyzed by [Rh(nbd){κ*P,N*-Ph$_2$P(CH$_2$)$_3$NMe$_2$}][BF$_4$]

The polymerization reactions were monitored by gas chromatography at regular time intervals, using octane as internal standard, which allowed to obtain time-conversion profiles showing the conversion of the corresponding monomer as a function of time. The influence of the electronic effects due to the substituent in *para* position can be analyzed in Fig. 5, which shows the time-conversion profiles for the polymerization of **PAa**, **PAb**, **PAc**, **PAd** and **PAe**. Phenylacetylene deriva-
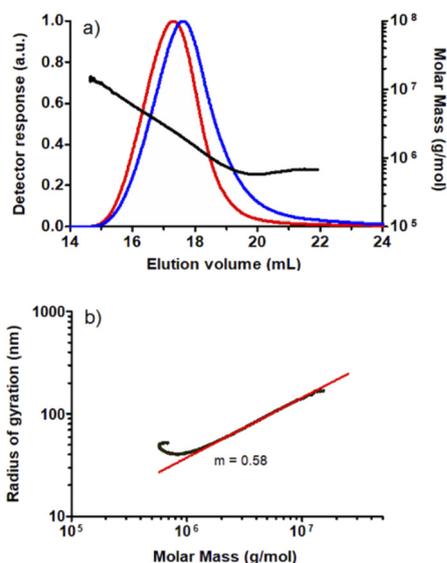

Fig. 3 (a) SEC chromatograms: light scattering detector response (90 degrees) (red) and differential refractometer response (blue), MM (molar mass) *vs.* elution volume plot for a **PPAe** sample prepared from **PAe** (R = *p*-OMe). (b) Log–log plot of the radius of gyration (r_g) *vs.* MM.
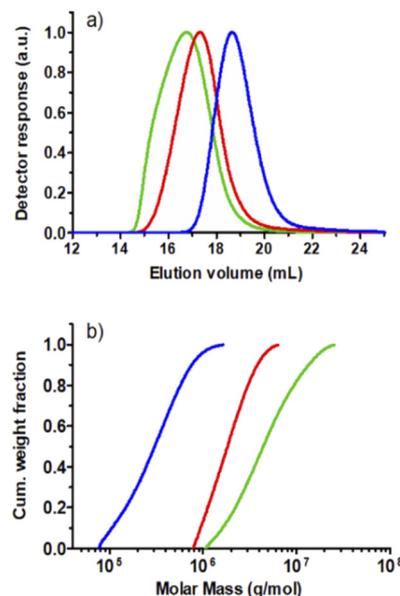

Fig. 4 (a) SEC chromatograms: light scattering detector response (90 degrees) and (b) Cumulative molar mass distribution plots for polymers: **PPAi** (green), **PPAe** (red) and **PPAh** (blue).
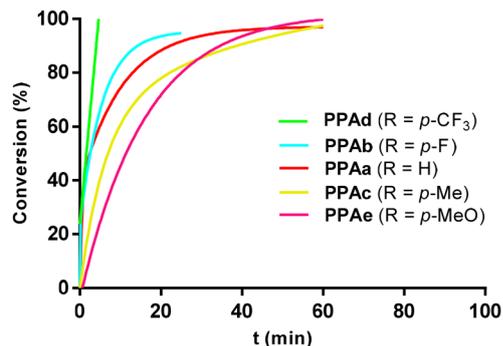
Fig. 5 Time-conversion plots for the polymerization of ring-substituted phenylacetylene derivatives. Reaction conditions: THF, 20 °C, $[PA]_o$ = 0.25 M, $[PA]_o/[Rh]$ = 100.

Fig. 6 Time-conversion plots for the polymerization of ring-substituted phenylacetylene derivatives. Reaction conditions: THF, 20 °C, $[PA]_o$ = 0.25 M, $[PA]_o/[Rh]$ = 100.
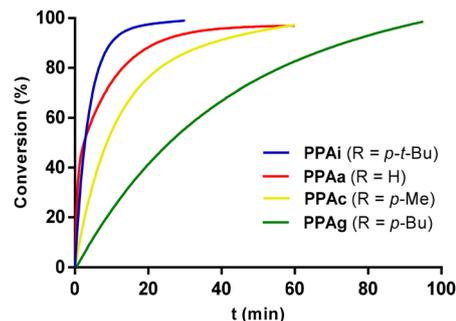
tives with an electron-withdrawing substituent in *para* position polymerized faster than phenylacetylene (**PAa**). The fastest polymerizing substituted phenylacetylene derivatives were **PAd** (R = *p*-CF$_3$) and **PAb** (R = *p*-F), which reached full conversion in 5 and 30 min, respectively. Monomer **PAc** (R = *p*-Me), with an electro-donating substituent, showed lower activity than phenylacetylene (**PAa**) although both reached full conversion in 60 min. The slowest polymerizing alkyne in this series was **PAe** (R = *p*-OMe) with lower conversions at short reaction times.

In principle, the presence of electron-withdrawing substituents on the aromatic ring should increase the acidity of the alkyne, favoring the initiation step by facilitating its deprotonation in route to the active alkynyl species (see below).[46] Indeed, the following pK_a values: *p*-nitrophenylacetylene, 17.98; *p*-fluorophenylacetylene, 18.14; phenylacetylene, 18.50; and *p*-methylphenylacetylene, 18.60; are fully consistent with the inductive effect predictions.[47,48] Accordingly, the calculated initiation efficiency in the polymerization of **PAb** (R = *p*-F), 1.8%, is slightly higher than that calculated for phenylacetylene (**PAa**, 0.9%) and 1-ethynyl-4-methoxybenzene (**PAe**, 0.6%). However, the influence of electronic effects on the chain propagation step, due to the reduced coordinative ability of the triple bond because of the attracting character of the substituent, has also been proposed.[25] The key role of acidity for homogeneous Rh (diene)-type catalysts is also evidenced by the lack of activity in polymerization of alkyl-acetylenes, which are much less acidic than the aryl-acetylene derivatives.[49] The catalyst also has a decisive influence on the activity in the polymerization of ring-substituted phenylacetylenes. In the case of the [Rh(tfb)(PPh$_3$)$_2$]$^+$/^{i}PrNH$_2$ catalytic system, electron-withdrawing groups decrease the catalytic activity and renders living polymerization difficult.[50] Interestingly, a positive correlation between the acidity of the ethynyl group, the catalytic activity and the polymer molar mass has been observed in the polymerization of ring-substituted phenylacetylene derivatives with *para*-substituted aromatic Schiff bases as pendant groups using the molecular catalyst [Rh(μ-OMe)(cod)]$_2$ or Rh(ɪ)/MCM41 supported catalysts, which suggests that the monomer acidity might play a substantial role also in the propagation step.[51,52]

The time-conversion profiles for the polymerization of monomers **PAc**, **PAg** and **PAi**, have enable the analysis of the influence of steric effects resulting from the substituent, as they all contain electron-donating alkyl groups at the *para* position (Fig. 6). **PAc** (R = *p*-Me) polymerized faster than **PAg** (R = *p*-Bu), as would be expected for the smaller methyl substituent. **PAc** achieved 33% conversion after 4 min, whereas **PAg** required 15 min to achieve 30% conversion. The polymerization of both alkynes was slower than that of phenylacetylene (**PAa**), which is consistent with the presence of electron-donating groups in the *para* position and the bulkiness of the *n*-butyl group. Unexpectedly, the polymerization of **PAi** (R = *p*-^{t}Bu) proceeded very quickly, despite having a very bulky substituent, achieving full conversion in just 30 min. In contrast, full conversion of **PAg** (R = *p*-Bu) took 95 min. It is worth noting that the spherical shape of *tert*-butyl compared to the tail shape of the flexible *n*-butyl substituent may facilitate the alkyne insertion throughout the propagation step of the polymerization process, resulting in faster polymerization rate. Also, the compactness plots representing the ratio between the hydrodynamic radius (r_h) and radius of gyration (r_g) *versus* elution volume,[53] showed that **PPAi** (R = *p*-^{t}Bu) has a compact spherical shape with a much denser core ($r_h(v)/r_g$ < 0.72) than **PPAg** (R = *p*-Bu) and **PPAa** (R = H) ($r_h(v)/r_g$ < 0.77) (see the ESI†). The lower value of $r_h(v)/r_g$ for **PPAi**, indicates a more compact polymer with a smaller volume, which is expected to facilitate the polymer propagation step. In this context, it should be noted that effective Rh(ɪ) catalysts have been described for the polymerization of **PAi** (R = *p*-^{t}Bu),[25,50] among which the catalyst [(η^6-C$_6$H$_5$-BPh$_3$)Rh(tfb)] stands out, achieving full conversion in 16 min using a $[PA]_o/[Rh]$ ratio of 500.[54] However, the molar mass of the polymer, M_n = 6.3 × 10^4, was much lower than that obtained with our catalyst [Rh(nbd){κ^{2}P, N-Ph$_2$P(CH$_2$)$_3$NMe$_2$}]$^+$.

On the other hand, ring-substituted phenylacetylene derivatives with an alkyl (–R) substituent polymerized faster than the corresponding alkoxy (–OR) derivatives, consistent with the strong electron-donating ability of the later. The observed order of activity was: **PAc** (R = *p*-Me) > **PAe** (R = *p*-OMe) > **PAf** (R = *m*-OMe). Similarly, **PAg** (R = *p*-Bu) polymerized faster than

PAh (R = *p*-OBu), although the latter exhibited a very limited activity, reaching only 40% conversion in 60 min (see the ESI†). On the other hand, the slow polymerization rate of **PAc** at high conversions (Fig. 5) should be a consequence of the insolubility of **PPAc**, which precipitates in the reaction medium, making the polymerization more difficult.

The first-order kinetic plots for the polymerizations of PA derivatives showed a linear dependence up to almost quantitative conversion in most cases, indicating that the concentration of the propagating species does not change during the polymerization, which indicates the absence of significant termination reactions,[55,56] as illustrated for **PAg** (R = *p*-Bu) in Fig. 7a. However, in some cases such as **PAc** (R = *p*-Me) and **PAh** (R = *p*-OBu), the line slightly deviates from the origin due to a relatively fast polymerization rate in the early stage of the reaction.[57] This is particularly relevant in the case of **PAa**, for which a 40% conversion was achieved after 1 min, with a decrease in activity after 5 min. It should be noted that for **PAb** (R = *p*-F) and **PAi** (R = *p*-ᵗBu) the plots deviate from linearity after reaching around 80% conversion due to the slowing down of the polymerization reaction (see the ESI†). Finally, a slight induction period of approximately 1 min was observed in the polymerization of the monomers **PAe** (R = *p*-OMe) (Fig. 7b) and **PAf** (R = *m*-OMe) for which negligible active species are present.

Thermal properties of polymers

Thermal properties of the PPA polymers were investigated by differential scanning calorimetry (DSC) and thermogravimetric analysis (TGA). The DSC thermograms (exo-down plots)
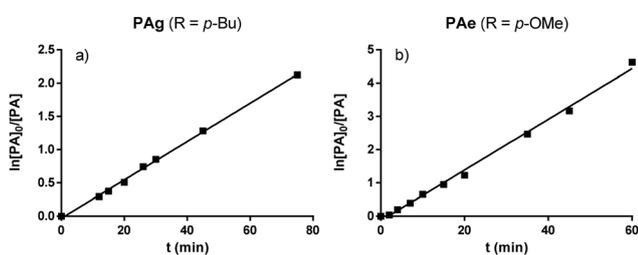

Fig. 7 Pseudo first-order kinetic plots for the polymerization of substituted phenylacetylene derivatives: (a) **PAg** (R = *p*-Bu) and (b) **PAe** (R = *p*-OMe). Reaction conditions: THF, T = 20 °C, $[PA]_o$ = 0.25 M, $[PA]_o/[Rh]$ = 100.

showed an exothermic peak in the first heating cycle that was not detected in the subsequent scan. As no thermal decomposition was observed in the TGA curve within this temperature range (see below), this irreversible peak could be attributed to exothermic polymer reactions such as *cis–trans* isomerization or the cross-linking of polymer chains. This peak, centered between 160–170 °C, is similar to that observed in other PPA samples and was ascribed to *cis–trans* isomerization of the main chain structure.[58] The isomerization temperature is not strongly influenced by either the nature or the position of the substituent, as it was observed slightly above 160 °C for all the PPA samples (Table 2), similar to poly(phenylacetylene). The exothermic peak is sharp in the case of **PPAa** (R = H), **PPAb** (R = *p*-F), **PPAe** (R = *p*-OMe) and **PPAf** (R = *m*-OMe), but this peak is broader for **PPAg** (R = *p*-Bu) and **PPAi** (R = *p*-ᵗBu) (Fig. 8). This result suggests that polymers with larger groups have stiffer chains, making thermal geometric isomerization more difficult.[59]

Thermal degradation of the polymers also occurs in solution. ¹H NMR monitoring of a solution of **PPAe** (R = *p*-OMe) in
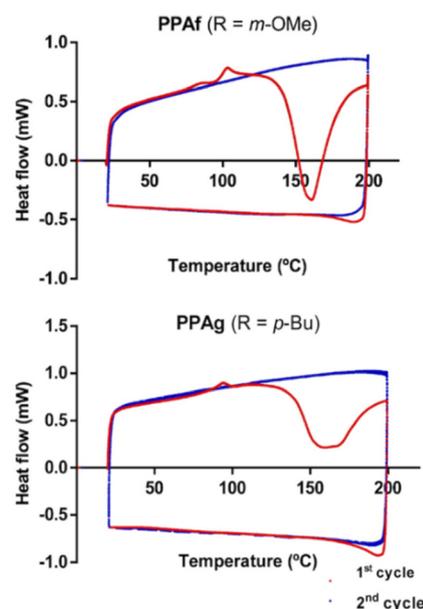

Fig. 8 DSC thermograms of polymer samples **PPAf** (R = *m*-OMe) and **PPAg** (R = *p*-Bu) in two consecutive heating/cooling cycles (10 °C min⁻¹).

Table 2 Thermal properties of the PPAs derived from TGA and DSC

Polymer	$T_{5\%}{}^{a}$ (°C)	$T_{onset}{}^{b}$ (°C)	$T_{max}{}^{c}$ (°C)	Other (°C)^{d}	Exothermic procces (°C)
PPAb (R = *p*-F)	273	286	374	—	167
PPAe (R = *p*-OMe)	297	325	424	369	163
PPAf (R = *m*-OMe)	304	325	408	368	161
PPAg (R = *p*-Bu)	314	351	432	393	161
PPAi (R = *p*-ᵗBu)	338	383	430	—	165

^{a} $T_{5\%}$: temperature for which the weight loss is 5%. ^{b} T_{onset}: onset of the decomposition processes. ^{c} T_{max}: temperature of the maximum in the weight loss rate. ^{d} Other maxima in the derivative thermogram.
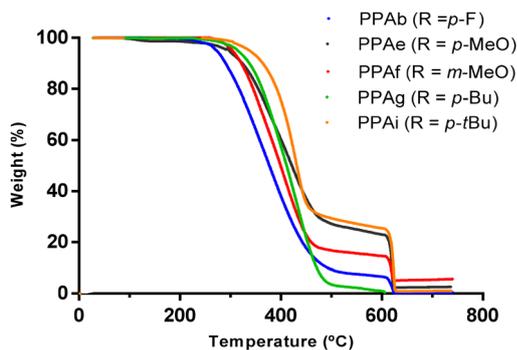
Fig. 9 TGA thermograms of PPA samples obtained from different monosubstituted phenylacetylenes.

toluene-d_8 showed evidence of polymer degradation after heating at 100 °C. In fact, a decrease in the intensity of the signals corresponding to the protons of the polymer main chain was observed after heating the solution for 10 min. In addition, analysis of the aromatic region of the spectrum recorded after heating at 100 °C for 90 min revealed the formation of a small amount of 1,3,5-triphenylbenzene (see the ESI†).[60]

The TGA curves of selected ring-substituted PPA polymers are shown in Fig. 9. The temperatures corresponding to 5% weight losses are in the range 270–340 °C ($T_{5\%}$). The most thermally stable polymer was **PPAi** (R = p-^{t}Bu), whose degradation temperature is 383 °C, while the least stable was **PPAb** (R = p-F) with a temperature of 286 °C (T_{onset}). On the other hand, polymer **PPAg** (R = p-Bu), also with a bulky substituent, showed a high decomposition temperature of 351 °C. Considering the temperature of the maximum weight loss rate (T_{max}), corresponding to a turning point of the weight loss curve, the PPAs with bulkier substituents, **PPAi** (R = p-^{t}Bu) and **PPAg** (R = p-Bu), showed the highest temperatures, together with **PPAe** (R = p-OMe). Polymers **PPAe–PPAg** also exhibited local maxima at slightly lower temperatures (Table 2).

The thermal decomposition process produces a significant weight loss up to about 500 °C with slight weight losses at higher temperature. At temperatures below 600 °C polymers **PPAi** (R = p-^{t}Bu) and **PPAe** (R = p-OMe) showed the highest residue (24%) while polymer **PPAg** (R = p-Bu) was completely degraded at this temperature. The polymers degrade above 600 °C on air generating residues of less than 5% by weight. The thermal behavior of substituted PPAs is comparable to that exhibited by poly(phenylacetylene).[35] However, bulky substituents have been found to improve the thermal stability of the polymers, as evidenced by the higher decomposition temperature.

Mechanistic considerations: the role of the hemilabile ligand

Studies of PA polymerization by rhodium(I) initiators have shown that the presence of an external base as co-catalyst, such as 4-(dimethylamino)pyridine (DMPA) or ^{i}PrNH$_2$, often improves catalyst performance by increasing initiation

efficiency[22,50,61] or inhibiting catalyst deactivation.[62] Mechanistic investigations on PA polymerization by the catalyst precursor [Rh(cod){$\kappa^2 P,N$-Ph$_2$P(CH$_2$)$_3$NMe$_2$}]$^+$ led us to observe the alkynyl species [Rh(C≡C–Ph)(cod){κP-Ph$_2$P(CH$_2$)$_3$NHMe$_2$}]$^+$ formed by the intramolecular proton transfer from a η^2-alkyne ligand to the –NMe$_2$ group, which acts as an internal base (Fig. 10a). In addition, mechanistic studies on PA polymerization by 2-diphenylphosphinopyridine-based rhodium(I) catalysts have allowed us to disclose the key role of rhodium-alkynyl species such as [Rh(C≡CPh)(cod)(κP-Ph$_2$PPy)] in the polymerization reaction.[23]

This cationic alkynyl intermediates may be involved in the initiation step, which likely entails the PA insertion into the Rh–alkynyl bond, through a four-membered transition state (not shown) to afford a stable rhodium-vinyl species responsible for the propagation step by successive PA coordination–insertion reactions with 2,1-regioselectivity (Fig. 10b). In this regard, related alkynyl species have been suggested to be the initiating species likely involved in the generation of stable rhodium–vinyl species, responsible for the propagation step.[32,50,63] Theoretical studies by Morokuma et al. with catalyst [Rh(nbd)(C≡C–Ph)(PA)] have shown that PA insertion into the Rh–alkynyl bond is possible as initiation step. In fact, the energy barrier for the PA insertion into the Rh–alkynyl bond (initiation step) is almost 4 kcal mol^{-1} higher than the barrier for the insertion into the Rh–vinyl bond (propagation step), which explains the low initiation efficiency (0.6–2%) observed in the polymerization of ring-substituted phenylacetylene derivatives.[64]
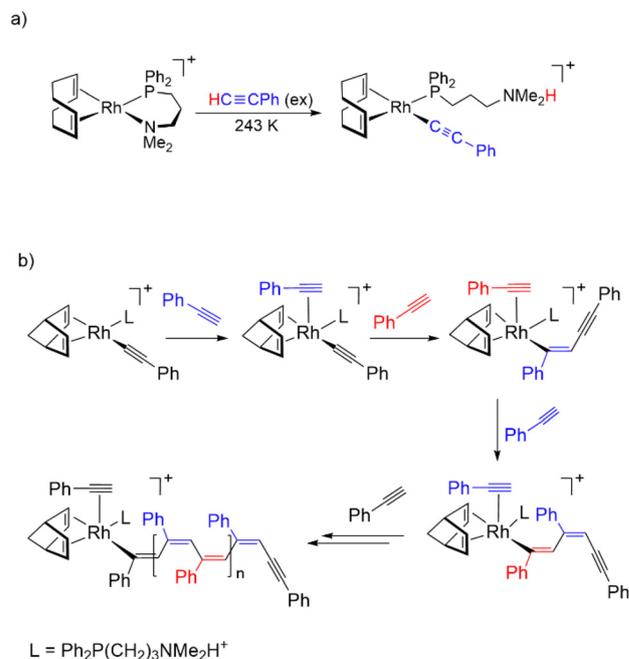

Fig. 10 (a) Formation of a Rh-alkynyl species triggered by a hemilabile phosphine ligand. (b) Plausible mechanism for the polymerization of ring-substituted PAs.

The low initiation efficiencies for the polymerization of ring-substituted phenylacetylene derivatives suggest that the activation of the catalysts to the alkynyl active species (Fig. 10a) does not determine the differences in the polymerization activity. Therefore, the electronic effects imparted by the substituent seem to influence the chain propagation step, which is faster for phenylacetylene derivatives with electron-withdrawing substituents on the aromatic ring.

Conclusions

The cationic compound [Rh(nbd){κ^2P,N-Ph$_2$P(CH$_2$)$_3$NMe$_2$}][BF$_4$] efficiently catalyzes the polymerization of a series of *para*- and *meta*-substituted phenylacetylene derivatives with groups of different electronic and steric properties to afford highly stereoregular ring-substituted poly(phenylacetylene)s with a *cis*-transoidal configuration of very high molar mass, M_w in the range 3.1×10^5–4.8×10^6, and moderate dispersities. Megadalton PPAs have been obtained in the polymerization of phenylacetylene and 1-ethynyl-3-methoxybenzene ($M_n \approx 1.1 \times 10^6$). Notably, the polymerization of 1-ethynyl-4-methoxybenzene and 1-(*tert*-butyl)-4-ethynylbenzene yields ultra-high molecular weight PPAs with M_n of 1.70×10^6 and 2.72×10^6, respectively. SEC-MALS analysis of the ring-substituted PPAs evidences the formation of linear PPAs unlike poly(phenylacetylene) whose conformational plot is consistent with the presence of high molar mass branched material. A correlation between the electronic properties of the substituent and the polymerizing activity has been observed. Phenylacetylene derivatives with an electron-withdrawing substituent in *para* position polymerize faster than phenylacetylene, whereas derivatives with an electron-donating substituent polymerize more slowly. Since the initiation efficiency is very low for both types of ring-substituted alkynes (<2%), the difference in activity should be related to the electronic effects in the chain propagation step. Phenylacetylene derivatives with bulky long chain substituents in *para* position polymerize at a slower rate than phenylacetyene. In contrast, the polymerization of 1-(*tert*-butyl)-4-ethynylbenzene is very fast and gives an ultra-high molecular weight PPA.

Author contributions

Marta Angoy: Investigation, methodology. M. Victoria Jiménez: Conceptualization, supervision, validation. Eugenio Vispe: Investigation, validation, visualization. Jesús J. Pérez-Torrente: Funding acquisition, conceptualization, supervision, writing – original draft, writing – review & editing.

Data availability

Data available upon request from the authors.

Conflicts of interest

There are no conflicts to declare.

Acknowledgements

References

1 R. M. Pankow and B. C. Thompson, The development of conjugated polymers as the cornerstone of organic electronics, *Polymer*, 2020, **207**, 122874.

2 P. Palania and S. Karpagam, Conjugated polymers – a versatile platform for various photophysical, electrochemical and biomedical applications: a comprehensive review, *New J. Chem.*, 2021, **45**, 19182–19209.

3 H. Lu, X. Li and Q. Lei, Conjugated Conductive Polymer Materials and its Applications: A Mini-Review, *Front. Chem.*, 2021, **9**, 732132.

4 J. W. Lam and B. Z. Tang, Functional polyacetylenes, *Acc. Chem. Res.*, 2005, **38**, 745–754.

5 T. Masuda, Substituted Polyacetylenes: Synthesis, Properties, and Functions, *Polym. Rev.*, 2017, **57**, 1–14.

6 L. Liu, Y. Zang, H. Jia, T. Aoki, T. Kaneko, S. Hadano, M. Teraguchi, M. Miyata, G. Zhang and T. Namikoshi, Helix-Sense-Selective Polymerization of Achiral Phenylacetylenes and Unique Properties of the Resulting Cis-cisoidal Polymers, *Polym. Rev.*, 2017, **57**, 89–118.

7 A. Xu, T. Masuda and A. Zhang, Stimuli-Responsive Polyacetylenes and Dendronized Poly(phenylacetylene)s, *Polym. Rev.*, 2017, **57**, 138–158.

8 R. Sakai, T. Satoh and T. Kakuchi, Polyacetylenes as Colorimetric and Fluorescent Chemosensor for Anions, *Polym. Rev.*, 2017, **57**, 159–174.

9 F. Freire, E. Quiñoá and R. Riguera, Supramolecular Assemblies from Poly(phenylacetylene)s, *Chem. Rev.*, 2016, **116**, 1242–1271.

10 D. T. Gentekos, R. J. Sifri and B. P. Fors, Controlling polymer properties through the shape of the molecular-weight distribution, *Nat. Rev. Mater.*, 2019, **4**, 761–774.

11 K. Nomura, S. Pengoubol and W. Apisuk, Synthesis of ultra-high molecular weight polymers by homopolymerisation of higher α-olefins catalysed by aryloxo-modified half-titanocenes, *RSC Adv.*, 2016, **6**, 16203–16207.

12 A. Reyhani, S. Allison-Logan, H. Ranji-Burachaloo, T. G. McKenzie, G. Bryant and G. G. Qiao, Synthesis of ultra-high molecular weight polymers by controlled pro-

duction of initiating radicals, *J. Polym. Sci., Part A: Polym. Chem.*, 2019, **57**, 1922–1930.

13 L. Zhang, X. Ren, Y. Zhang and K. Zhang, Step-Growth Polymerization Method for Ultrahigh Molecular Weight Polymers, *ACS Macro Lett.*, 2019, **8**, 948–954.

14 K. Patel, S. H. Chikkali and S. Sivaram, Ultrahigh molecular weight polyethylene: Catalysis, structure, properties, processing and applications, *Prog. Polym. Sci.*, 2020, **109**, 101290.

15 J. Liu, J. W. Lam and B. Z. Tang, Acetylenic polymers: syntheses, structures, and functions, *Chem. Rev.*, 2009, **109**, 5799–5867.

16 M. Shiotsuki, F. Sanda and T. Masuda, Polymerization of substituted acetylenes and features of the formed polymers, *Polym. Chem.*, 2011, **2**, 1044–1058.

17 M. A. Casado, A. Fazal and L. A. Oro, Rhodium-Catalyzed Polymerization of Phenylacetylene and its Derivatives, *Arabian J. Sci. Eng.*, 2013, **38**, 1631–1646.

18 J. Sedláček and H. Balcar, Substituted Polyacetylenes Prepared with Rh Catalysts: From Linear to Network-Type Conjugated Polymers, *Polym. Rev.*, 2017, **57**, 31–51.

19 M. Isomura, Y. Misumi and T. Masuda, Living polymerization and block copolymerization of various ring-substituted phenylacetylenes by rhodium-based ternary catalyst, *Polym. Bull.*, 2000, **45**, 335–339.

20 J. Sedláček and J. Vohlídal, Controlled and living polymerizations induced with rhodium catalysts. A review, *Collect. Czech. Chem. Commun.*, 2003, **68**, 1745–1790.

21 N. S. L. Tan and A. B. Lowe, Polymerizations Mediated by Well-Defined Rhodium Complexes, *Angew. Chem., Int. Ed.*, 2020, **59**, 5008–5021.

22 Y. Kishimoto, P. Eckerle, T. Miyatake, M. Kainosho, A. Ono, T. Ikariya and R. Noyori, Well-controlled polymerization of phenylacetylenes with organorhodium(I) complexes: Mechanism and structure of the polyenes, *J. Am. Chem. Soc.*, 1999, **121**, 12035–12044.

23 M. Angoy, M. V. Jiménez, F. J. Modrego, L. A. Oro, V. Passarelli and J. J. Pérez-Torrente, Mechanistic Investigation on the Polymerization of Phenylacetylene by 2-Diphenyl-phosphinopyridine Rhodium(I) Catalysts: Understanding the Role of the Cocatalyst and Alkynyl Intermediates, *Organometallics*, 2018, **37**, 2778–2794.

24 I. Saeed, M. Shiotsuki and T. Masuda, Living Polymerization of Phenylacetylene with Tetrafluorobenzobarrelene Ligand-Containing Rhodium Catalyst Systems Featuring the Synthesis of High Molecular Weight Polymer, *Macromolecules*, 2006, **39**, 8567–8573.

25 N. Onishi, M. Shiotsuki, T. Masuda, N. Sano and F. Sanda, Polymerization of Phenylacetylenes Using Rhodium Catalysts Coordinated by Norbornadiene Linked to a Phosphino or Amino Group, *Organometallics*, 2013, **32**, 846–853.

26 N. S. L. Tan, P. V. Simpson, G. L. Nealon, A. N. Sobolev, P. Raiteri, M. Massi, M. I. Ogden and A. B. Lowe, Rhodium (I)-α-Phenylvinylfluorenyl Complexes: Synthesis, Characterization, and Evaluation as Initiators in the Stereospecific Polymerization of Phenylacetylene, *Eur. J. Inorg. Chem.*, 2019, 592–601.

27 N. S. L. Tan, G. L. Nealon, J. M. Lynam, A. N. Sobolev, M. R. Rowless, M. I. Ogden, M. Massi and A. B. Lowe, A (2-(naphthalen-2-yl)phenyl)rhodium(I) complex formed by a proposed intramolecular 1,4-ortho-to-ortho′ Rh metal-atom migration and its efficacy as an initiator in the controlled stereospecific polymerisation of phenylacetylene, *Dalton Trans.*, 2019, **48**, 16437–16447.

28 N. S. L. Tan, G. L. Nealon, G. F. Turner, S. A. Moggach, M. I. Ogden, M. Massi and A. B. Lowe, Rh(I)(2,5-norbornadiene)(biphenyl)(*tris*(4-fluorophenyl)phosphine): Synthesis, Characterization, and Application as an Initiator in the Stereoregular (Co)Polymerization of Phenylacetylenes, *ACS Macro Lett.*, 2020, **9**, 56–60.

29 T. Taniguchi, T. Yoshida, K. Echizen, K. Takayama, T. Nishimura and K. Maeda, Facile and Versatile Synthesis of End-Functionalized Poly(phenylacetylene)s: A Multicomponent Catalytic System for Well-Controlled Living Polymerization of Phenylacetylenes, *Angew. Chem., Int. Ed.*, 2020, **59**, 8670–8680.

30 W. Yang, M. Tabata, S. Kobayashi, K. Yokota and A. Shimizu, Synthesis of Ultra-High-Molecular-Weight Aromatic Polyacetylenes with [Rh(norbornadiene)Cl]₂-Triethylamine and Solvent-Induced Crystallization of the Obtained Amorphous Polyacetylenes, *Polym. J.*, 1991, **23**, 1135–1138.

31 T. Tang, S. J. Lu, G. Ahumada and C. W. Bielawski, Megadalton Macromolecules Made-to-Order in Minutes: A Highly Active Nanosphere Catalys for Preparing High-Molecular Weight Polymers, *Macromolecules*, 2022, **55**, 9943–9950.

32 M. Angoy, M. V. Jiménez, P. García-Orduña, L. A. Oro, E. Vispe and J. J. Pérez-Torrente, Dinuclear Phosphine-Amido [Rh₂(diene){μ-NH(CH₂)₃PPh₂}₂] Complexes as Efficient Catalyst Precursors for Phenylacetylene Polymerization, *Organometallics*, 2019, **38**, 1991–2006.

33 M. V. Jiménez, J. J. Pérez-Torrente, M. I. Bartolomé, E. Vispe, F. J. Lahoz and L. A. Oro, Branched Poly(phenylacetylene), *Macromolecules*, 2010, **43**, 6278–6283.

34 M. Angoy, M. V. Jiménez, F. J. Lahoz, E. Vispe and J. J. Pérez-Torrente, Polymerization of phenylacetylene catalyzed by rhodium(I) complexes with N-functionalized N-heterocyclic carbene ligands, *Polym. Chem.*, 2022, **13**, 1411–1421.

35 M. V. Jiménez, J. J. Pérez-Torrente, M. I. Bartolomé, E. Vispe, F. J. Lahoz and L. A. Oro, Cationic rhodium complexes with hemilabile phosphine ligands as polymerization catalyst for high molecular weight stereoregular poly (phenylacetylene), *Macromolecules*, 2009, **42**, 8146–8156.

36 M. V. Jiménez, J. J. Pérez-Torrente, M. I. Bartolomé and L. A. Oro, Convenient Methods for the Synthesis of a Library of Hemilabile Phosphines, *Synthesis*, 2009, 1916–1922.

37 J. Sedlácek, J. Vohlídal and Z. Grubisic-Gallot, Molecular–weight determination of poly(phenylacetylene) by size–

exclusion chromatography/low–angle laser light scattering. influence of polymer degradation, *Makromol. Chem., Rapid Commun.*, 1993, **14**, 51–53.

38 V. Percec and J. G. G. Rudick, Independent electrocyclization and oxidative chain cleavage along the backbone of cis-poly(phenylacetylene), *Macromolecules*, 2005, **38**, 7241–7250.

39 S. Podzimek, *Light Scattering, Size Exclusion Chromatography and Asymmetric Flow Field Flow Fractionation*, John Wiley and Sons, Hoboken, New Jersey, 2011, pp. 65–72.

40 A. Furlani, C. Napoletano, M. V. Russo and W. Feast, Stereoregular polyphenylacetylene, *J. Polym. Bull.*, 1986, **16**, 311–317.

41 A. Furlani, C. Napoletano, M. V. Russo, A. Camus and N. J. Marsich, The influence of the ligands on the catalytic activity of a series of RhI complexes in reactions with phenylacetylene: Synthesis of stereoregular poly(phenyl) acetylene, *J. Polym. Sci., Part A: Polym. Chem.*, 1989, **27**, 75–86.

42 Y. Kishimoto, M. Itou, T. Miyatake, T. Ikariya and R. Noyori, Polymerization of monosubstituted acetylenes with a zwitterionic rhodium(I) complex, $Rh^+(2,5\text{-norbornadiene})[\eta^6\text{-}C_6H_5)B(C_6H_5)_3]$, *Macromolecules*, 1995, **28**, 6662–6666.

43 A. Miyasaka, T. Sone, Y. Mawatari, S. Setayesh, K. Müllen and M. Tabata, Poly[(para-halogenated)phenylacetylene]s Prepared with a [Rh(norbornadiene)Cl]₂ Catalyst: Syntheses and Structure Elucidation, *Macromol. Chem. Phys.*, 2006, **207**, 1938–1944.

44 W. Yun-Hua and F. Tsai, Reusable Rhodium(I)/Cationic Bipyridyl-catalyzed Polymerization of Phenylacetylenes in Water under Aerobic Conditions, *Chem. Lett.*, 2007, **36**, 1492–1493.

45 C. Cametti, P. Codastefano, R. D'Amato, A. Furlani and M. V. Russo, Static and dynamic light scattering measurements of polyphenylacetylene (PPA) in different organic solvents (tetrahydrofuran, toluene and chloroform), *Synth. Met.*, 2000, **114**, 173–179.

46 A. Escudero, R. Vilar, R. Salcedo and T. Ogawa, Effects of substituent groups and substituted benzenes on the polymerization of phenylacetylenes initiated by di-μ-pentafluorothiophenolatebis(1,5-cyclooctadiene)-rhodium(I), *Eur. Polym. J.*, 1995, **31**, 1135–1138.

47 J. O. Stoffer, D. R. Strait, D. L. Filger, E. T. Lloyd and C. Crain, A novel method for direct measurement of the pKa's of weakly acidic hydrocarbons, *J. Org. Chem.*, 1978, **43**, 1812–1813.

48 E. T. Lloyd, *Part I: Thermodynamic acidities of substituted phenylacetylenes*, Missouri University of Science and Technology, USA, 1976. https://scholarsmine.mst.edu/20masters_theses/5998.

49 O. Trhlíková, J. Zedník, H. Balcar, J. Brus and J. Sedláček, [Rh(cycloolefin)(acac)] complexes as catalysts of polymerization of aryl- and alkylacetylenes: Influence of cycloolefin ligand and reaction conditions, *J. Mol. Catal. A: Chem.*, 2013, **378**, 57–66.

50 M. Shiotsuki, N. Onishi, F. Sanda and T. Masuda, Living polymerization of phenylacetylenes catalyzed by cationic rhodium complexes bearing tetrafluorobenzobarrelene, *Polym. J.*, 2011, **43**, 51–57.

51 H. Balcar, J. Sedláček, J. Zedník, V. Blechta, P. Kubát and J. Vohlídal, Polymerization of isomeric N-(4-substituted benzylidene)-4-ethynylanilines and 4-substituted N-(4- ethynylbenzylidene)anilines by transition metal catalysts: preparation and characterization of new substituted polyacetylenes with aromatic Schiff base type pendant groups, *Polymer*, 2001, **42**, 6709–6721.

52 H. Balcar, J. Sedláček, J. Čejka and J. Vohlídal, MCM–41–Immobilized [Rh(cod)OCH₃]₂ Complex – A Hybrid Catalyst for the Polymerization of Phenylacetylene and Its Ring–Substituted Derivatives, *Makromol. Chem., Rapid Commun.*, 2002, **23**, 32–37.

53 A. K. Brewer and A. M. Striegel, Characterizing the Size, Shape, and Compactness of a Polydisperse Prolate Ellipsoidal Particle via Quadruple-Detector Hydrodynamic Chromatography, *Analyst*, 2011, **136**, 515–519.

54 N. Onishi, M. Shiotsuki, F. Sanda and T. Masuda, Polymerization of Phenylacetylenes with Rhodium Zwitterionic Complexes: Enhanced Catalytic Activity by π-Acidic Diene Ligands, *Macromolecules*, 2009, **42**, 4071–4076.

55 Y. Misumi, K. Kanki, M. Miyake and T. Masuda, Living polymerization of phenylacetylene by rhodium-based ternary catalysts, (diene)Rh(I) complex/vinyllithium/phosphorus ligand. Effects of catalyst components, *Macromol. Chem. Phys.*, 2000, **201**, 2239–2244.

56 N. S. L. Tan, G. L. Nealon, S. A. Moggach, J. M. Lynam, M. I. Ogden, M. Massi and A. B. Lowe, (η4−Tetrafluorobenzobarrelene)−η¹−((tri-4-fluorophenyl)phosphine)−η¹−(2-phenylphenyl)rhodium(I): A Catalyst for the Living Polymerization of Phenylacetylenes, *Macromolecules*, 2021, **54**, 6191–6203.

57 M. Shiotsuki, N. Onishi, F. Sanda and T. Masuda, Living Polymerization of Phenylacetylene Catalyzed by a Cationic Rh Complex Bearing Tetrafluorobenzobarrelene, *Chem. Lett.*, 2010, **39**, 244–245.

58 M. Goto, M. Minami, H. Sogawaa and F. Sanda, Reinvestigation of thermal isomerization of cis-stereoregulated poly(phenylacetylene) by spectroscopic study and DFT calculation, *Polymer*, 2021, **229**, 124013.

59 Y. Fujita, Y. Misumi, M. Tabata and T. Masuda, Synthesis, geometric structure, and properties of poly(phenylacetylenes) with bulky para-substituents, *J. Polym. Sci., Part A: Polym. Chem.*, 1998, **36**, 3157–3163.

60 O. Trhlíková, J. Zedník, J. Vohlídal and J. Sedlácek, Molecular weight and configurational stability of poly (phenylacetylene) prepared with Rh catalyst, *Polym. Degrad. Stab.*, 2011, **96**, 1310–1320.

61 Y. Kishimoto, T. Miyatake, T. Ikariya and R. Noyori, An efficient rhodium(I) initiator for stereospecific living polymerization of phenylacetylenes, *Macromolecules*, 1996, **29**, 5054–5055.

62 H. Komatsu, Y. Suzuki and H. Yamazaki, Unprecedented rhodium-mediated tetramerization of bulky terminal alkynes leading to hydropentalenylrhodium complexes, *Chem. Lett.*, 2001, **30**, 998–999.

63 Y. Tian, X. Li, J. Shi, B. Tonga and Y. Dong, Monomer-induced switching of stereoselectivity and limitation of chain growth in the polymerization of amine-containing para-substituted phenylacetylenes by [Rh(norbornadiene)Cl]$_2$, *Polym. Chem.*, 2017, **8**, 5761–5768.

64 Z. Ke, S. Abe, T. Ueno and K. Morokuma, Rh-catalyzed Polymerization of Phenylacetylene: Theoretical Studies of the Reaction Mechanism, Regioselectivity, and Stereoregularity, *J. Am. Chem. Soc.*, 2011, **133**, 792–7941.